High accuracy splitting algorithms for the time-dependent Schrödinger equation with a train of laser pulses

A.A. Gusev, O. Chuluunbaatar, S.I. Vinitsky,
Joint Institute of Nuclear Research, Russia,
and M.S. Kaschiev
Institute of Mathematics and Informatics, Bulgarian Academy of Science, Bulgaria

ABSTRACT

High accuracy splitting algorithms based on the unitary approximations of the evolution operator for the time-dependent Schrödinger equation (TDSE) with a train of laser pulses are developed. The efficiency of the algorithms is shown using typical examples of a hydrogen atom affected by a train of laser pulses in the dipole approximation and an additional constant magnetic field. The stabilization effects are discussed.

Keywords: Splitting algorithms, Schrödinger equation, unitary approximations, evolution operator, atoms interacting with laser pulses

1. INTRODUCTION

Numerical solutions of the TDSE have found wide application in different quantum mechanical problems and modern laser physics experiments. In particular, these experiments stimulate computer modeling of the dynamics of exotic few-body Coulomb systems affected by a train of laser pulses[1-3] . In this case a possibility of constructing efficient splitting algorithms appeared[3-5] . There are two requirements for the numerical methods developed, namely, they should be stable and have high accuracy in both time and space variables.

In the present paper we formulate two methods for solving the TDSE that provide second- and forth-order approximation in the time step based on the unitary splitting algorithms[6,7] . The finite-element method is used to construct numerical schemes of arbitrary accuracy in the spatial step[8-11] . As examples we consider the models of the two-dimensional oscillator in an ac electric field and Coulomb-like atoms in a constant magnetic field and a train of short laser pulses.

2. STATEMENT OF THE PROBLEM AND GENERAL CALCULATION SCHEMES

Let us consider the initial problem for the multidimensional TDSE describing the dynamics of a model atom in the external field in the time interval $t \in [t_0, T]$

$$i\frac{\partial\psi(\vec{r},t)}{\partial t} = H(\vec{r},t)\psi(\vec{r},t), \quad \psi(\vec{r},t_0) = \psi_0(\vec{r}), \quad \psi(\vec{r},t) \in \mathbf{H^1(R^n)} \times [\mathbf{t_0, T}], \quad \psi_0(\vec{r}) \in \mathbf{H^1(R^n)}, \tag{1}$$

where

$$H(\vec{r},t) = H_0(\vec{r}) + Q(\vec{r},t), \quad \text{with} \quad H_0(\vec{r}) = -\frac{1}{2}\Delta_{\vec{r}} + V(\vec{r}). \tag{2}$$

Here $H_0(\vec{r})$ is the Hamiltonian of a free atom with the continuous potential $V(\vec{r})$, and the time dependent potential function $Q(\vec{r},t)$ describes the interaction of the free atom with the external field $\vec{F}(t)$ in the dipole approximation $Q(\vec{r},t) = \vec{r}\vec{F}(t)$. The normalization condition looks as

$$||\psi|| = \int |\psi(\vec{r},t)|^2 d\vec{r} = 1, \quad t \in [t_0, T]. \tag{3}$$

Further author information:
S.I.V: E-mail: vinitsky@thsun1.jinr.ru

Saratov Fall Meeting 2003: Laser Physics and Photonics, Spectroscopy, and Molecular Modeling,
edited by V. L. Derbov, L. A. Melnikov, L. M. Babkov, Proceedings of SPIE Vol. 5476
(SPIE, Bellingham, WA, 2004) · 0277-786X/04/$15 · doi: 10.1117/12.578913

Let us consider the formulated problem (1) on the uniform grid $\Omega_\tau = \{t_0, t_{k+1} = t_k + \tau, k = 0, 1, ...K, t_K = T\}$, with the time step τ. The solution $\psi(t_{k+1}) \equiv \psi(\vec{r}, t_{k+1})$ is expressed in terms of the solution $\psi(t_k)$ by means of the unitary evolution operator $U(t, t_0)$,

$$\psi(t_{k+1}) = U(t_{k+1}, t_k)\psi(t_k). \tag{4}$$

The unitary operator $U(t_{k+1}, t_k)$ can be represented in the following way[6] :

$$U(t_{k+1}, t_k) = \lim_{N\to\infty} U^{(N)}(t_{k+1}, t_k), \quad U^{(N)}(t_{k+1}, t_k) = \exp\left(-i\tau G_k^N\right), \quad -i\tau G_k^N = \sum_{j=1}^{N} \tau^j A_j^k(\tau), \tag{5}$$

where $A_j^k(\tau)$ is the anti-Hermitian operator which consists of multiple integrals of commutators of the Hamiltonian $H(\vec{r}, t)$ at different moments of time . For $N = 1$ one has the known Crank-Nicholson scheme with the truncation error $O(\tau^2)$ with respect to the time step τ,

$$\left(I + \frac{\tau}{2} i\, G_k^1\right)\psi^{k+1} = \left(I - \frac{\tau}{2} i\, G_k^1\right)\psi^k, \quad ||\psi^{k+1}|| = ||\psi^k||, \tag{6}$$

with

$$G_k^1 = H(\vec{r}, t_{k+1/2}), \quad \psi^0 = \psi(\vec{r}, t_0), \quad t_{k+1/2} = t_k + \frac{\tau}{2}. \tag{7}$$

As it is well known[6] , for $N = 2$ the operator G_k^2 has the form

$$G_k^2 = H(\vec{r}, t_{k+1/2}) + \frac{\tau^2}{24}\frac{\partial^2 Q(\vec{r}, t_{k+1/2})}{\partial t^2} - i\frac{\tau^2}{12}\left(\frac{1}{2}\left(\Delta_{\vec{r}}\frac{\partial Q(\vec{r}, t_{k+1/2})}{\partial t}\right) + \left(\vec{\nabla}\frac{\partial Q(\vec{r}, t_{k+1/2})}{\partial t}\right)\vec{\nabla}\right). \tag{8}$$

Here we used the Taylor-series of $Q(\vec{r}, t)$ in the vicinity of the point $t_{k+1/2}$ with the truncation error $O(\tau^4)$ with respect to the time step τ. By means of the following transformation:

$$\begin{aligned} &G_k^2 \exp\left(-\frac{i\tau^2}{12}\frac{\partial Q(\vec{r}, t_{k+1/2})}{\partial t}\right)\psi(t_k) = \exp\left(-\frac{i\tau^2}{12}\frac{\partial Q(\vec{r}, t_{k+1/2})}{\partial t}\right)\hat{G}_k^2\psi(t_k) + O(\tau^4), \\ &\hat{G}_k^2 = H(\vec{r}, t_{k+1/2}) + \frac{\tau^2}{24}\frac{\partial^2 Q(\vec{r}, t_{k+1/2})}{\partial t^2}, \end{aligned} \tag{9}$$

we can replace the operator G_k^2 with simpler operator $\hat{G}_k^2$. From here with the help of the Padé approximation for the unitary operator $U(t_{k+1}, t_k)$ we have an implicit two-ply scheme with the truncation error $O(\tau^4)$ with respect to the time step τ,

$$\begin{cases} \Psi^k = \exp\left(\dfrac{i\tau^2}{12}\dfrac{\partial Q(\vec{r}, t_{k+1/2})}{\partial t}\right)\psi^k, \\ \left(I - \dfrac{\tau}{4}\alpha\hat{G}_k^2\right)\Psi^{k+1/2} = \left(I - \dfrac{\tau}{4}\alpha^*\hat{G}_k^2\right)\Psi^k, \\ \left(I + \dfrac{\tau}{4}\alpha^*\hat{G}_k^2\right)\Psi^{k+1} = \left(I + \dfrac{\tau}{4}\alpha\hat{G}_k^2\right)\Psi^{k+1/2}, \\ \psi^{k+1} = \exp\left(-\dfrac{i\tau^2}{12}\dfrac{\partial Q(\vec{r}, t_{k+1/2})}{\partial t}\right)\Psi^{k+1}, \end{cases} \quad ||\psi^{k+1}|| = ||\Psi^{k+1/2}|| = ||\psi^k||, \tag{10}$$

where $\Psi^{k+1/2}$ is an auxiliary function and $\alpha = 1/\sqrt{3} - i$.

We apply these schemes to exactly and not exactly solvable models for showing their efficiency and stability.

2.1. Exactly solvable model: two-dimensional oscillator

The TDSE for a two-dimensional oscillator (or a charged particle in a constant uniform magnetic field) in the external governing electric field with the components $E_1(t)$ and $E_2(t)$ not equal to zero in the finite time interval $t \in (0, T]$ in the dipole approximation and atomic units has the form[12]

$$\begin{aligned} i\frac{\partial}{\partial t}\phi(x,y,t) = -\frac{1}{2}\left(\frac{\partial^2}{\partial x^2}+\frac{\partial^2}{\partial y^2}\right)\phi(x,y,t) + \frac{i\omega}{2}\left(x\frac{\partial}{\partial y}-y\frac{\partial}{\partial x}\right)\phi(x,y,t) \\ +\frac{\omega^2}{8}(x^2+y^2)\phi(x,y,t) - (xE_1(t)+yE_2(t))\phi(x,y,t). \end{aligned} \tag{11}$$

The transformation to the coordinate frame rotating with the frequency $\omega/2$

$$x = x_1\cos\left(\frac{\omega t}{2}\right) + y_1\sin\left(\frac{\omega t}{2}\right), \quad y = y_1\cos\left(\frac{\omega t}{2}\right) - x_1\sin\left(\frac{\omega t}{2}\right) \tag{12}$$

leads to the following equation

$$\begin{aligned} i\frac{\partial}{\partial t}\phi(x_1,y_1,t) = -\frac{1}{2}\left(\frac{\partial^2}{\partial x_1^2}+\frac{\partial^2}{\partial y_1^2}\right)\phi(x_1,y_1,t) + \frac{\omega^2}{8}(x_1^2+y_1^2)\phi(x_1,y_1,t) \\ +(f_1(t)x_1 + f_2(t)y_1)\phi(x_1,y_1,t), \end{aligned} \tag{13}$$

where

$$f_1(t) = -E_1(t)\cos\left(\frac{\omega t}{2}\right) + E_2(t)\sin\left(\frac{\omega t}{2}\right), \quad f_2(t) = -E_1(t)\sin\left(\frac{\omega t}{2}\right) - E_2(t)\cos\left(\frac{\omega t}{2}\right). \tag{14}$$

In the polar coordinates

$$x_1 = r\cos(\theta), \quad y_1 = r\sin(\theta), \quad \theta \le 0 < 2\pi \tag{15}$$

this equation has the form

$$\begin{aligned} i\frac{\partial}{\partial t}\phi(r,\theta,t) = -\frac{1}{2}\left(\frac{1}{r}\frac{\partial}{\partial r}r\frac{\partial}{\partial r}+\frac{1}{r^2}\frac{\partial^2}{\partial\theta^2}\right)\phi(r,\theta,t) + \frac{\omega^2 r^2}{8}\phi(r,\theta,t) \\ +(f_1(t)\cos(\theta) + f_2(t)\sin(\theta))r\phi(r,\theta,t). \end{aligned} \tag{16}$$

Using the Galerkin projection of the solutions by means of the basis of the angular functions $D_j(\theta)$

$$\phi(r,\theta,t) = \sum_{j=0}^{N-1}\chi_j(r,t)D_j(\theta), \tag{17}$$

where

$$D_0(\theta) = \frac{1}{\sqrt{2\pi}}, \quad D_{2j}(\theta) = \frac{1}{\sqrt{\pi}}\cos(j\,\theta), \quad D_{2j-1}(\theta) = \frac{1}{\sqrt{\pi}}\sin(j\,\theta), \quad j > 0, \tag{18}$$

we arrive at a set of ordinary differential equations for unknown coefficients $\{\chi_j(r,t)\}_{j=0}^{N-1}$ in the interval $t \in [0, T]$

$$\begin{aligned} i\frac{\partial}{\partial t}\chi_j(r,t) = \sum_{k=0}^{N-1}\left(-\delta_{kj}\frac{1}{2}\frac{1}{r}\frac{\partial}{\partial r}r\frac{\partial}{\partial r} + H_{jk}(r,t)\right)\chi_k(r,t), \\ \lim_{r\to 0} r\frac{\partial}{\partial r}\chi_j(r,t) = 0 \text{ and } \chi_j(r_{max},t) = 0, \end{aligned} \tag{19}$$

with

$$H_{jk}(r,t)=\begin{cases}\dfrac{\omega^2 r^2}{8}+\dfrac{1}{2r^2}\left[\dfrac{j+1}{2}\right]^2, & j=k,\\ \dfrac{r}{\sqrt{2}}f_2(t), & \min(j,k)=0,\quad \max(j,k)=1,\\ \dfrac{r}{\sqrt{2}}f_1(t), & \min(j,k)=0,\quad \max(j,k)=2,\\ \dfrac{r}{2}f_2(t), & \mathrm{mod}(\min(j,k),2)=0 \text{ and } \max(j,k)=\min(j,k)+1,\\ -\dfrac{r}{2}f_2(t), & \mathrm{mod}(\min(j,k),2)=1 \text{ and } \max(j,k)=\min(j,k)+3,\\ \dfrac{r}{2}f_1(t), & \mathrm{mod}(j-k,2)=0,\\ 0, & \text{otherwise.}\end{cases} \tag{20}$$

The initial functions $\chi_j(r,t)$ at $t=0$ (in the case $f_1(0)=f_2(0)=0$) are chosen in the form

$$\chi_0(r,0)=\sqrt{\omega}\exp\left(-\frac{1}{4}\omega r^2\right),\quad \chi_j(r,0)\equiv 0,\quad j>0. \tag{21}$$

The transformation to the projective variable, $\rho: r=R(t)\rho$, and to the envelope, $\xi_j(\rho,t)$, of the solutions[4,7]

$$\chi_j(r,t)=\frac{1}{R(t)}\exp\left\{\frac{i}{2}R(t)\frac{dR(t)}{dt}\rho^2\right\}\xi_j(\rho,t) \tag{22}$$

reduces the above set of equations (19) to the following one:

$$\begin{aligned} &i\frac{\partial}{\partial t}\xi_j(\rho,t)=\sum_{k=0}^{N-1}\left(-\delta_{jk}\frac{1}{2R^2(t)}\,\frac{1}{\rho}\frac{\partial}{\partial\rho}\rho\frac{\partial}{\partial\rho}+H_{jk}^{(0)}(\rho,t)\right)\xi_k(\rho,t),\\ &\lim_{\rho\to 0}\rho\frac{\partial}{\partial\rho}\xi_j(\rho,t)=0 \text{ and } \xi_j(\rho_{max},t)=0,\end{aligned} \tag{23}$$

where

$$H_{jj}^{(0)}(\rho,t)=H_{jj}(\rho,t)+\frac{1}{2}R(t)\frac{d^2R(t)}{dt^2}\rho^2,\quad H_{jk}^{(0)}(\rho,t)=H_{jk}(\rho,t),\quad j\neq k. \tag{24}$$

Note, that this representation provides some appropriate localization and smoothness of the envelope by the projective variable. For this problem we use the Crank-Nicholson scheme and the formula (6) is rewritten on the uniform grid $\Omega_{\delta t}$

$$A(\rho,t_{k+1/2})\xi(\rho,t_{k+1})=A^*(\rho,t_{k+1/2})\xi(\rho,t_k), \tag{25}$$

where

$$A_{jk}(\rho,t_{k+1/2})=\delta_{jk}+\frac{\delta t}{2}i\left(-\delta_{jk}\frac{1}{2R^2(t_{k+1/2})}\,\frac{1}{\rho}\frac{\partial}{\partial\rho}\rho\frac{\partial}{\partial\rho}+H_{jk}^{(0)}(\rho,t_{k+1/2})\right), \tag{26}$$

and $\xi(\rho,t)=(\xi_0(\rho,t),\ldots\xi_{N-1}(\rho,t))^T$.

The exact solution of Eq. (13) reads

$$\phi_{ext}(x_1,y_1,t)=\sqrt{\frac{\omega}{2\pi}}\exp\left(-A_1(t)x_1^2-A_2(t)y_1^2+2B_1(t)x_1+2B_2(t)y_1-C_1(t)-C_2(t)\right), \tag{27}$$

where the functions $A_j(t)$, $B_j(t)$, $C_j(t)$, $j=1,2$ satisfy the Cauchy problem

$$\begin{aligned} &i\frac{d}{dt}A_j(t)=2A_j^2(t)-\frac{\omega^2}{8}, && A_j(0)=\frac{\omega}{4},\\ &i\frac{d}{dt}B_j(t)=2A_j(t)B_j(t)+\frac{f_j(t)}{2}, && B_j(0)=0,\\ &i\frac{d}{dt}C_j(t)=-A_j(t)+2B_j^2(t), && C_j(0)=0.\end{aligned} \tag{28}$$

Here the exact solution of the first differential equation is $A_j(t) \equiv \omega/4$ in the whole time interval $t \in [0, T]$.

Note, that this problem has an exact solution for a particular choice of the field $E_{1,2}(t) = a_{1,2} \sin \omega_{1,2} t$ which provides a good test example to examine the efficiency of the numerical algorithms and the rate of convergence of the projection with respect to the number N of radial equations and to the time T. The needed projections of the exact solution onto the radial ones have the form

$$\chi_j^{ext}(r,t) = \int_0^{2\pi} D_j(\theta) \phi_{ext}(r,\theta,t) d\theta. \tag{29}$$

We compare some numerical results with the exact ones in Section 4.1.

2.2. Model not solvable exactly: a three-dimensional Coulomb atom

As it is known, δ-shaped pulses are a widely used approximation for electric-field pulses that are much shorter than the classical orbital period. The Hamiltonian of the kicked hydrogen atom in atomic units[13] has the form

$$H = H_0 + V_{ext}, \quad \text{with} \quad H_0 = -\frac{1}{2}\Delta_{\vec{r}} - \frac{1}{r}, \quad V_{ext} = \vec{r}\,\vec{F} \sum_{k=1}^{S} \delta(t - kT), \tag{30}$$

where S is the number of kicks applied, T is the period, and $\vec{F}$ is the external field.

Between the pulses we have a conservative system and the wave packet propagates in correspondence with the simple field-free conservative Hamiltonian H_0 of the hydrogen atom, i.e., the wave packet evolves according to the time-dependent Schrödinger equation

$$i \frac{\partial \psi(\vec{r},t)}{\partial t} = H_0 \psi(\vec{r},t), \quad \psi(\vec{r},t) \in \mathbf{H^1(R^3)} \times [\mathbf{(k-1)T, kT}]. \tag{31}$$

If the field direction is the same for all pulses, e.g., along the z axis, the system has rotational symmetry with respect to this axis and, hence, the corresponding component (here the z- component) of the angular momentum is conserved. The electric field causes strong coupling of bound states to the continuum leading to ionization. This is the main computational challenge, which, however, can be straightforwardly mastered by means of space-discretization methods. Due to the discretization, the wave packet will not be approximated by a globally defined basis or by bound states and thus the well-known problem of finding suitable bases is "simply" reduced, first, to selecting sufficiently large coordinate space, which allows wave packet propagation without reflection at the borders, and, second, to selecting suitable interpolation polynomials on the space grid.

The formal solution for the time development of the discretized wave functions $\psi(t) \equiv \psi(\vec{r},t)$ evolving under the time-independent Hamiltonian is given by

$$\psi(t + \delta t) = \exp(-i\, H_0 \delta t) \psi(t). \tag{32}$$

Inserting (10) into (32) leads to an implicit system of algebraic equations

$$\begin{aligned} \left(I - \frac{\delta t}{4} \alpha H_0\right) \hat{\psi} &= \left(I - \frac{\delta t}{4} \alpha^* H_0\right) \psi(t), \\ \left(I + \frac{\delta t}{4} \alpha^* H_0\right) \psi(t + \delta t) &= \left(I + \frac{\delta t}{4} \alpha H_0\right) \hat{\psi}, \end{aligned} \tag{33}$$

which have to be solved for each time step δt. Here $\hat{\psi}$ is an auxiliary function.

To explain the computational procedure for periodic δ pulses, we restrict the discussion below to the Schrödinger equation for a single pulse directed along the z axis

$$i \frac{\partial \psi(\vec{r},t)}{\partial t} = (H_0 + \vec{r}\,\vec{F}\,\delta(t - T)) \psi(\vec{r},t). \tag{34}$$

Several pulses are then simply computed by repeating the computational steps described below for a single pulse. Thus, the same method allows also one to describe systems with non-periodic, randomly distributed pulses, pulses of varying strength, or pulses directed in the opposite directions.

We use the following expressions for expressing the wave function $\psi(\vec{r}, T_+)$ directly after the pulse $t = T_+$

$$\psi(\vec{r}, T_+) = \exp\left(-i\, H_0(T_+ - T_-) - i\, \vec{r}\vec{F} \int_{T_-}^{T_+} \delta(t-T)dt\right) \psi(\vec{r}, T_-), \tag{35}$$

via the wave function $\psi(\vec{r}, T_-)$ just before the pulse. From here, obviously, $T_+ - T_- \to 0$ and $\int_{T_-}^{T_+} \delta(t-T)dt \equiv 1$. Hence, the formula (35) is equivalent to the formula

$$\psi(\vec{r}, T_+) = \exp\left(-i\, \vec{r}\vec{F}\right) \psi(\vec{r}, T_-). \tag{36}$$

For practical calculations we used the analogous formulae (33)

$$\begin{aligned} \left(I - \frac{1}{4}\alpha\, \vec{r}\vec{F}\right) \hat{\psi} &= \left(I - \frac{1}{4}\alpha^* \vec{r}\vec{F}\right) \psi(T_-), \\ \left(I + \frac{1}{4}\alpha^* \vec{r}\vec{F}\right) \psi(T_+) &= \left(I + \frac{1}{4}\alpha\, \vec{r}\vec{F}\right) \hat{\psi} \end{aligned} \tag{37}$$

which preserve unitarity and are correct in order $(\vec{r}\vec{F})^4$ at finite $\vec{r} \in \Omega$ to formula (36).

After changing the variables by $r = n\rho$, $t = n^2\tau$ the equation (31) reads

$$i\, \frac{\partial \psi(\vec{\rho}, \tau)}{\partial \tau} = H_0 \psi(\vec{\rho}, \tau), \quad H_0 = -\frac{1}{2}\Delta_{\vec{\rho}} - \frac{n}{\rho}, \tag{38}$$

and Eqs. (37) look like

$$\begin{aligned} \left(I - \frac{n}{4}\alpha\, \vec{\rho}\vec{F}\right) \hat{\psi} &= \left(I - \frac{n}{4}\alpha^* \vec{\rho}\vec{F}\right) \psi(\hat{T}_-), \\ \left(I + \frac{n}{4}\alpha^*\, \vec{\rho}\vec{F}\right) \psi(\hat{T}_+) &= \left(I + \frac{n}{4}\alpha\, \vec{\rho}\vec{F}\right) \hat{\psi} \end{aligned} \tag{39}$$

where $\hat{T} = T/n^2$ and n is the principle quantum number.

For a linearly polarized laser field the solution reads

$$\psi(\vec{\rho}, \tau) = \sum_{l=0}^{l_{max}} \chi_l^n(\rho, \tau) Y_l^0(\theta, \phi), \tag{40}$$

where Y_l^m is a spherical function. After the substitution (40) the equation (38) is equivalent to a set of equations

$$i\, \frac{\partial \chi_l^n(\rho, \tau)}{\partial \tau} = \sum_{l'=0}^{l_{max}} \left(-\delta_{ll'} \frac{1}{2} \frac{1}{\rho^2} \frac{\partial}{\partial \rho} \rho^2 \frac{\partial}{\partial \rho} + H_{ll'}^{(0)}(\rho)\right) \chi_{l'}^n(\rho, \tau), \tag{41}$$

with the boundary conditions

$$\lim_{\rho \to 0} \rho^2 \frac{\partial}{\partial \rho} \chi_l^n(\rho, \tau) = 0 \text{ and } \chi_l^n(\rho_{max}, \tau) = 0. \tag{42}$$

In this case the formulae (33) and (39) on the uniform grid $\Omega_{\delta\tau}$ take the form

$$\begin{aligned} B(\rho)\hat{\chi}^n &= B^*(\rho)\chi^n(\rho, \tau_k), \qquad B_{ll'}(\rho) = \delta_{ll'} - \frac{\delta\tau}{4}\alpha \left(-\delta_{ll'} \frac{1}{2} \frac{1}{\rho^2} \frac{\partial}{\partial \rho} \rho^2 \frac{\partial}{\partial \rho} + H_{ll'}^{(0)}(\rho)\right), \\ C^*(\rho)\chi^n(\rho, \tau_{k+1}) &= C(\rho)\hat{\chi}^n, \quad C_{ll'}(\rho) = \delta_{ll'} + \frac{\delta\tau}{4}\alpha \left(-\delta_{ll'} \frac{1}{2} \frac{1}{\rho^2} \frac{\partial}{\partial \rho} \rho^2 \frac{\partial}{\partial \rho} + H_{ll'}^{(0)}(\rho)\right), \end{aligned} \tag{43}$$

and

$$A(\rho)\hat{\chi}^n = A^*(\rho)\chi^n(\rho,\hat{T}_-), \quad A_{ll'}(\rho) = \delta_{ll'} - \frac{1}{4}\alpha H^{(1)}_{ll'}(\rho),$$
$$D^*(\rho)\chi^n(\rho,\hat{T}_+) = D(\rho)\hat{\chi}^n, \quad D_{ll'}(\rho) = \delta_{ll'} + \frac{1}{4}\alpha H^{(1)}_{ll'}(\rho), \tag{44}$$

where the matrix elements $H^{(0)}_{ll'}$ and $H^{(1)}_{ll'}$ can be written as

$$H^{(0)}_{ll'}(\rho) = \left(\frac{l(l+1)}{2\rho^2} - \frac{n}{\rho}\right)\delta_{ll'}, \; H^{(1)}_{ll'}(\rho) = n\rho F\frac{\sqrt{(2l+1)(2l'+1)}}{2}\frac{l+l'+1}{(l+l'+1)^2-1}\delta_{1,|l-l'|}, \tag{45}$$

and $\chi^n(\rho,\tau) = (\chi^n_0(\rho,\tau),...,\chi^n_{l_{max}}(\rho,\tau))^T$.

The initial state is given by

$$\chi^n_l(\rho,0) = N_l R_{nl}(\rho), \tag{46}$$

where

$$R_{nl}(\rho) = \frac{2(2\rho)^l\exp(-\rho)}{\sqrt{n}(2l+1)!}\sqrt{\frac{(n+l)!}{(n-l-1)!}}\,{}_1F_1\left(-n+l+1, 2l+2, 2\rho\right), \tag{47}$$

N_l are the normalized constants, and ${}_1F_1$ is the confluence hypergeometric function. We used the following orthogonal transformation between the parabolic and hydrogen states

$$\Phi^{(0)}_{n_1n_2m}(\mathbf{y}) = \sum_{l=|m|}^{n-1} A^{n_1n_2}_{nlm}\Phi^{(0)}_{nlm}(\mathbf{y}), \qquad \Phi^{(0)}_{nlm}(\mathbf{y}) = \sum_{n_1,n_2=0}^{n-|m|} A^{n_1n_2}_{nlm}\Phi^{(0)}_{n_1n_2m}(\mathbf{y}). \tag{48}$$

Here the matrix elements A read[14]

$$A^{n_1n_2}_{nlm} = C^{n_1n_2}_{nlm}\;\; {}_3F_2\left[\begin{array}{l} |m|+l+1, -l+|m|+1, -n_2; \quad 1 \\ |m|+1, -n+|m|+1, \end{array}\right], \tag{49}$$

where $C^{n_1n_2}_{nlm}$ is the normalization factor

$$C^{n_1n_2}_{nlm} = (-1)^{l-|m|}\frac{(n-|m|-1)!}{|m|!}\sqrt{\left[\frac{(2l+1)(l+|m|)!(n_1+|m|)!(n_2+|m|)!}{(n+l)!(l-|m|)!(n-l-1)!(n_1)!(n_2)!}\right]}, \tag{50}$$

and ${}_3F_2$ is the hypergeometric function.

For analytical evaluation of the wave package dynamics of the kicked hydrogen atom (34) we decompose the time-dependent wave function $\psi(\vec{r},t)$ in the basis of the eigenfunctions $\psi_\lambda = \psi_\lambda(\vec{r},0)$ of the Hamiltonian H_0 (31)

$$\psi(\vec{r},t) = \sum_\lambda \alpha_\lambda(t)\psi_\lambda, \quad H_0\psi_\lambda = E_\lambda\psi_\lambda, \tag{51}$$

where λ is the set of quantum numbers, $\alpha_\lambda(t)$ are the coefficients. Using (32), (36) and (51) one can easily find the equations for $\alpha_\lambda(t)$

$$\alpha_\lambda(t+\delta t) = \exp(-i\,E_\lambda\delta t)\alpha_\lambda(t), \tag{52}$$

$$\alpha_\lambda(kT_+) = \sum_{\lambda'}\langle\lambda|\exp(-i\vec{r}\vec{F})|\lambda'\rangle\alpha_{\lambda'}(kT_-) \equiv \sum_{\lambda'}\tilde{\alpha}_{\lambda\lambda'}\alpha_{\lambda'}(kT_-). \tag{53}$$

The matrix elements $\tilde{\alpha}_{\lambda\lambda'} = \langle\lambda|\exp(-i\vec{r}\vec{F})|\lambda'\rangle$ between the parabolic functions $\psi_{n_1,n_2,m}$ of a free hydrogen atom are known analytically[14] (the external field $\vec{F} = (0,0,F)$ is directed along z):

$$\tilde{\alpha}_{\lambda\lambda'} = \tilde{\alpha}_{n_1n_2mn_1'n_2'm'} \quad E_\lambda = E_{n_1n_2m} = \frac{1}{2(n_1+n_2+m+1)^2}. \tag{54}$$

Note that in the Eqs.(51) and (53) we summarize only the states with $n \le n_{max}$ and neglect the transitions to states with $n > n_{max}$. We do not consider transitions to the states of the continuous spectrum and neglect reverse transitions from the states of continuum to the discrete ones. The probability of a transition to the state with quantum numbers λ is equal to $|\alpha_\lambda(t)|^2$.

3. HIGH–ORDER APPROXIMATIONS OF THE FINITE–ELEMENT METHOD

The conventional substitution $\chi_\nu^n(\rho,\tau) = e^{-iE\tau}\chi_\nu(\rho)$ to the set of N equations (41) leads to the Sturm–Liouville problem on the finite interval $\rho \in [0, \rho_{max}]$ for evaluating the initial states $\chi_\nu^n(\rho,0) = \chi_\nu(\rho)$ and energy eigenvalues E

$$\begin{aligned} &\sum_{\nu=1}^{N}\left(-\delta_{\mu\nu}\frac{1}{2}\frac{1}{\rho^2}\frac{\partial}{\partial\rho}\rho^2\frac{\partial}{\partial\rho} + H_{\mu\nu}^{(0)}(\rho)\right)\chi_\nu(\rho) = E\chi_\mu(\rho), \\ &\lim_{\rho\to 0}\rho^2\frac{\partial}{\partial\rho}\chi_\mu(\rho) = 0 \text{ and } \chi_\mu(\rho_{max}) = 0 \end{aligned} \tag{55}$$

that is equivalent[8–11] to the following variational Rayleigh-Ritz functional (the prime means the differentiation in ρ):

$$R(\chi) = \frac{\sum_{\mu,\nu=1}^{N}\int_0^{\rho_{max}}\left[\frac{1}{2}\chi_\mu'(\rho)\chi_\nu'(\rho)\delta_{\mu\nu} + \chi_\mu(\rho)H_{\mu\nu}^{(0)}(\rho)\chi_\nu(\rho)\right]\rho^2 d\rho}{\sum_{\mu,\nu=1}^{N}\int_0^{\rho_{max}}\chi_\mu(\rho)\chi_\nu(\rho)\delta_{\mu\nu}\rho^2 d\rho}. \tag{56}$$

Computational schemes of the high order of accuracy are derived from the variational functional (15) on the basis of the finite-element method. The general idea of the finite element method[10,11] (FEM) in one-dimensional space is to subdivide the interval $[0, \rho_{\max}]$ into many small domains called elements. The size and shape of the elements can be defined very freely so that physical properties can be taken into account.

Now we cover the interval $\Delta = [0, \rho_{\max}]$ with a system of subintervals $\Delta_j = [\rho_{j-1}, \rho_j]$ in such a way that $\Delta = \bigcup_{j=1}^{n}\Delta_j$, where n is the number of subintervals. In each interval Δ_j determine the following nodes:

$$\rho_{j,r}^p = \rho_{j-1} + \frac{h_j}{p}r,\ r = 0,1,...,p-1,p, \tag{57}$$

and the Lagrange elements $\left\{\phi_{j,r}^p(\rho)\right\}_{r=0}^p$

$$\phi_{j,r}^p(\rho) = \frac{(\rho-\rho_{j,0}^p)(\rho-\rho_{j,1}^p)\cdots(\rho-\rho_{j,r-1}^p)(\rho-\rho_{j,r+1}^p)\cdots(\rho-\rho_{j,p}^p)}{(\rho_{j,r}^p-\rho_{j,0}^p)(\rho_{j,r}^p-\rho_{j,1}^p)\cdots(\rho_{j,r}^p-\rho_{j,r-1}^p)(\rho_{j,r}^p-\rho_{j,r+1}^p)\cdots(\rho_{j,r}^p-\rho_{j,p}^p)}. \tag{58}$$

By means of the Lagrange elements $\phi_{j,r}^p(\rho)$, at each node $\rho_{j,r}^p$ we define the function $N_l(\rho)$ in the the following way:

$$N_l(\rho) = \begin{cases} \begin{cases} \phi_{1,0}^p(\rho), & \rho\in\Delta_1, \\ 0, & \rho\notin\Delta_1, \end{cases} & l = 0, \\ \begin{cases} \phi_{j,r}^p(\rho), & \rho\in\Delta_j, \\ 0, & \rho\notin\Delta_j, \end{cases} & l = r + p(j-1),\ r = 1,2,...p-1, \\ \begin{cases} \phi_{j,p}^p(\rho), & \rho\in\Delta_j, \\ \phi_{j,0}^p(\rho), & \rho\in\Delta_{j+1}, \\ 0, & \rho\notin\Delta_j\bigcup\Delta_{j+1}, \end{cases} & l = jp,\ j = 1,2,...,n-1, \\ \begin{cases} \phi_{n,p}^p(\rho), & \rho\in\Delta_n, \\ 0, & \rho\notin\Delta_n, \end{cases} & l = np. \end{cases} \tag{59}$$

The functions $\{N_l^p(\rho)\}_{l=0}^L, L = np$ form a basis in the space of polynomials of the p-th order. We approximate each function $\chi_\mu(\rho)$ of the global function $\chi(\rho) \equiv (\chi_1(\rho), \chi_2(\rho), ..., \chi_N(\rho))^T$ by a finite sum of local functions $N_l^p(\rho)$

$$\chi_\mu(\rho) = \sum_{l=0}^{L}\chi_\mu^l N_l^p(\rho), \quad \chi_\mu^l \equiv \chi_\mu^l(\rho_{j,r}^p), \tag{60}$$

and substitute the expansion (60) into the functional (55). From the minimum condition[8,9] for this functional we obtain that the vector solution χ^h is an eigenvector of the generalized algebraic problem

$$\mathbf{K}^p \chi^h = E^h \mathbf{M}^p \chi^h. \tag{61}$$

The following estimations for FEM eigenfunctions of the problem (22) are valid[8]:

$$| E_j^h - E_j | \le c_1(E_j) h^{2p}, \tag{62}$$

$$\left\| \chi_j^h(\rho) - \chi_j(\rho) \right\| \le c_2(E_j) h^{p+1}, \tag{63}$$

where h is the maximal step of the finite–element grid, j is the number of the corresponding solution, and the constants c_1 and c_2 do not depend on the step h. The stiffness matrix $\mathbf{K}^p$ and the mass matrix $\mathbf{M}^p$ are symmetric and have band structure, and the $\mathbf{M}^p$ matrix is also positively defined. They have the following form:

$$\mathbf{K}^p = \sum_{j=1}^{n} \mathbf{k}_j^p, \quad \mathbf{M}^p = \sum_{j=1}^{n} \mathbf{m}_j^p, \tag{64}$$

where the local matrices $\mathbf{k}_j^p$ on the element Δ_j and $\mathbf{m}_j^p$ are defined by the formulae

$$\begin{aligned}
&(\mathbf{k}_j^p)_{\mu\nu}^{qr} = \int_{-1}^{+1} \left\{ \delta_{\mu\nu} \frac{2}{h_j^2} (\phi_{j,q}^p)'(\phi_{j,r}^p)' + H_{\mu\nu}^{(0)}(\rho) \phi_{j,q}^p \phi_{j,r}^p \right\} \rho^2 \frac{h_j}{2} d\eta, \\
&(\mathbf{m}_j^p)_{\mu\nu}^{qr} = \delta_{\mu\nu} \int_{-1}^{+1} \phi_{j,q}^p \phi_{j,r}^p \rho^2 \frac{h_j}{2} d\eta, \\
&\rho = \rho_{j-1} + 0.5 h_j (1+\eta), \quad q,r = 0,1,...,p, \quad \mu,\nu = 1,2,...,N.
\end{aligned} \tag{65}$$

Now let us denote by η_g and $w_g, g = 0,\dots,p$ the Gaussian[15] nodes and weights in the interval $\eta \in [-1,1]$. Then the integrals given above are calculated as

$$\begin{aligned}
&(\mathbf{k}_j^p)_{\mu\nu}^{qr} = \sum_{g=0}^{p} \left\{ \delta_{\mu\nu} \frac{2}{h_j^2} (\phi_{j,q}^p)'(\eta_g)(\phi_{j,r}^p)'(\eta_g) + H_{\mu\nu}^{(0)}(\rho_g) \phi_{j,q}^p(\eta_g) \phi_{j,r}^p(\eta_g) \right\} \rho_g^2 \frac{h_j}{2} w_g, \\
&(\mathbf{m}_j^p)_{\mu\nu}^{qr} = \delta_{\mu\nu} \sum_{g=0}^{p} \phi_{j,q}^p(\eta_g) \phi_{j,r}^p(\eta_g) \rho_g^2 \frac{h_j}{2} w_g,
\end{aligned} \tag{66}$$

where $\rho_g = \rho_{j-1} + 0.5 h_j (1+\eta_g)$.

The reduction of Eqs. (43) and (44) on the finite interval $\rho \in [0, \rho_{max}]$ with the Neumann boundary conditions using the above realization of the FEM in Galerkin's formulation[16] leads to the following computation scheme on the grid $\Omega_{\delta\tau}^{\hat{T}}(\tau \in [0, \tau_{max}])$:

$$\text{between kicks } \tau \in (\tau_k, \hat{T}) \qquad \begin{aligned}
&\left(\mathbf{M}^p - \frac{\delta\tau}{4} \alpha \mathbf{K}_0^p \right) \hat{\chi}^h = \left(\mathbf{M}^p - \frac{\delta\tau}{4} \alpha^* \mathbf{K}_0^p \right) \chi^h(\tau_k), \\
&\left(\mathbf{M}^p + \frac{\delta\tau}{4} \alpha^* \mathbf{K}_0^p \right) \chi^h(\tau_{k+1}) = \left(\mathbf{M}^p + \frac{\delta\tau}{4} \alpha \mathbf{K}_0^p \right) \hat{\chi}^h,
\end{aligned} \tag{67}$$

and

$$\text{at kick } \hat{T}_- \le \hat{T} \le \hat{T}_+ \qquad \begin{aligned}
&\left(\mathbf{M}^p - \frac{1}{4} \alpha \mathbf{K}_1^p \right) \hat{\chi}^h = \left(\mathbf{M}^p - \frac{1}{4} \alpha^* \mathbf{K}_1^p \right) \chi^h(\hat{T}_-), \\
&\left(\mathbf{M}^p + \frac{1}{4} \alpha^* \mathbf{K}_1^p \right) \chi^h(\hat{T}_+) = \left(\mathbf{M}^p + \frac{1}{4} \alpha \mathbf{K}_1^p \right) \hat{\chi}^h.
\end{aligned} \tag{68}$$

Here the matrices $\mathbf{M}^p$ and $\mathbf{K}_0^p$ are given by Eqs. (64)-(65) and the matrix $\mathbf{K}_1^p$ is defined in a similar way

$$\mathbf{K}_1^p = \sum_{j=1}^{n} \mathbf{k}_j^p, \tag{69}$$

where the local matrix $\mathbf{k}_j^p$ on the element Δ_j is defined by

$$(\mathbf{k}_j^p)_{\mu\nu}^{qr} = \int_{-1}^{+1} H_{\mu\nu}^{(1)}(\rho)\phi_{j,q}^p \phi_{j,r}^p \rho^2 \frac{h_j}{2} d\eta, \tag{70}$$

$$\rho = \rho_{j-1} + 0.5h_j(1+\eta), \quad q,r = 0,1,...,p, \quad \mu,\nu = 1,2,...,N.$$

These integrals are calculated by using the above notation for the Gaussian[15] nodes η_g and weights $w_g, g = 0,\ldots,p$ in the interval $[-1,1]$

$$(\mathbf{k}_j^p)_{\mu\nu}^{qr} = \sum_{g=0}^{p} H_{\mu\nu}^{(1)}(\rho_g)\phi_{j,q}^p(\eta_g)\phi_{j,r}^p(\eta_g)\rho_g^2 \frac{h_j}{2} w_g, \tag{71}$$

where $\rho_g = \rho_{j-1} + 0.5h_j(1+\eta_g)$. Here we calculate the matrices $\mathbf{M}^p$, $\mathbf{K}_0^p$ and $\mathbf{K}_1^p$ only once in the whole time interval $t \in [0,T]$.

We define the following auxiliary time-dependent function:

$$Er^2(t,j) = \sum_{\nu=1}^{N} \int_0^{\rho_{max}} [\chi_\nu(\rho,t) - \chi_\nu^{h_j}(\rho,t)]^* [\chi_\nu(\rho,t) - \chi_\nu^{h_j}(\rho,t)]\rho^2 d\rho, \tag{72}$$

where $\chi_\nu^{h_j}(\rho,t)$ is the numerical solution with the time step $h_j = \delta t/2^{j-1}$ and j=1,2,3. For the function $\chi_\nu(\rho,t)$ an approximate calculation with the time step $\delta t/8$ can be used. By means of the values $Er(t,j)$ we can calculate the convergence rate $\alpha(t)$ of the calculation schemes (67) and (68) by means of the formula

$$\alpha(t) = \log_2 \left| \frac{Er(t,1) - Er(t,2)}{Er(t,2) - Er(t,3)} \right|. \tag{73}$$

In this case we must use the number of the Gaussian nodes $p \geq 4$.

Remark: For the two-dimensional case (See Section 2.1, Eqs. (25) and (26)) we used the following Crank-Nicholson scheme on the uniform grid $\Omega_{\delta t}$:

$$\left(\mathbf{M}^p + \frac{\delta t}{2} i\, \mathbf{K}_0^p\right) \xi^h(t_{k+1}) = \left(\mathbf{M}^p - \frac{\delta t}{2} i\, \mathbf{K}_0^p\right) \xi^h(t_k), \tag{74}$$

and the matrices $\mathbf{k}_j^p$ and $\mathbf{m}_j^p$ are redefined as

$$\begin{aligned} (\mathbf{k}_j^p)_{\mu\nu}^{qr} &= \int_{-1}^{+1} \left\{ \delta_{\mu\nu} \frac{2}{R^2(t_{k+1/2})h_j^2} (\phi_{j,q}^p)'(\phi_{j,r}^p)' + H_{\mu\nu}^{(0)}(\rho, t_{k+1/2})\phi_{j,q}^p \phi_{j,r}^p \right\} \rho \frac{h_j}{2} d\eta, \\ (\mathbf{m}_j^p)_{\mu\nu}^{qr} &= \delta_{\mu\nu} \int_{-1}^{+1} \phi_{j,q}^p \phi_{j,r}^p \rho \frac{h_j}{2} d\eta. \end{aligned} \tag{75}$$

Note, that in this case at each moment t_k we must calculate the matrix elements $H_{\mu\nu}^{(0)}(\rho, t_{k+1/2})$, i.e., redefine the matrices $\mathbf{K}_0^p$. The formula (72) is also redefined

$$Er^2(t,j) = \sum_{\nu=1}^{N} \int_0^{\rho_{max}} [\xi_\nu(\rho,t) - \xi_\nu^{h_j}(\rho,t)]^* [\xi_\nu(\rho,t) - \xi_\nu^{h_j}(\rho,t)]\rho d\rho. \tag{76}$$

Table 1. The test results of the integral errors $Er(t)$ of Eq. (76). Here $N_{max} = N$ is the number of the differential equations used, T is the time interval (in atomic units), t is the time and $t_{run}(T)$ is the run time (in minutes) of the computer calculations up to T=5 at PC Pentium IV 2.4GHz, 512 MB Windows XP.

$N_{max} \setminus t$	0.2	1.0	2.0	3.0	4.0	5.0	$t_{run}(T)$
1	1.30(-4)	6.48(-2)	4.48(-1)	6.88(-1)	6.90(-1)	5.92(-1)	1
3	5.02(-7)	5.76(-3)	1.15(-1)	2.56(-1)	3.35(-1)	3.99(-1)	3
5	5.20(-8)	6.28(-4)	3.85(-2)	1.29(-1)	1.92(-1)	2.58(-1)	8
10	5.20(-8)	3.04(-6)	2.98(-3)	2.17(-2)	4.52(-2)	8.15(-2)	33
15	5.20(-8)	5.08(-7)	3.99(-5)	9.94(-4)	3.26(-3)	1.26(-2)	80
20	5.20(-8)	5.08(-7)	2.71(-6)	8.20(-5)	4.10(-4)	2.14(-3)	155
25	5.20(-8)	5.08(-7)	2.18(-6)	3.94(-6)	1.66(-5)	2.07(-4)	263

For the function $\xi_\nu(\rho, t)$ the exact solution can be used, see Eqs. (29) and (22).

Following this procedure we can formulate the following strategy: as we know analytically all functions $H^{(0)}_{\mu\nu}$ and $H^{(1)}_{\mu\nu}$ we first choose the FEM grid, then we calculate the matrix elements at the Gaussian points and finally evaluate the integrals. This allow us to organize the calculation scheme as follows: let us consider the system of N equations. We evaluate the values of all matrix elements for these N equations at the Gaussian nodes and store them in the external file.

From the above estimates one can see that we have a very high accuracy calculating the eigenvalues, the bound states, and the corresponding wave functions. From this point of view the main error in the solution depends only on the number of equations N and the computer precision used.

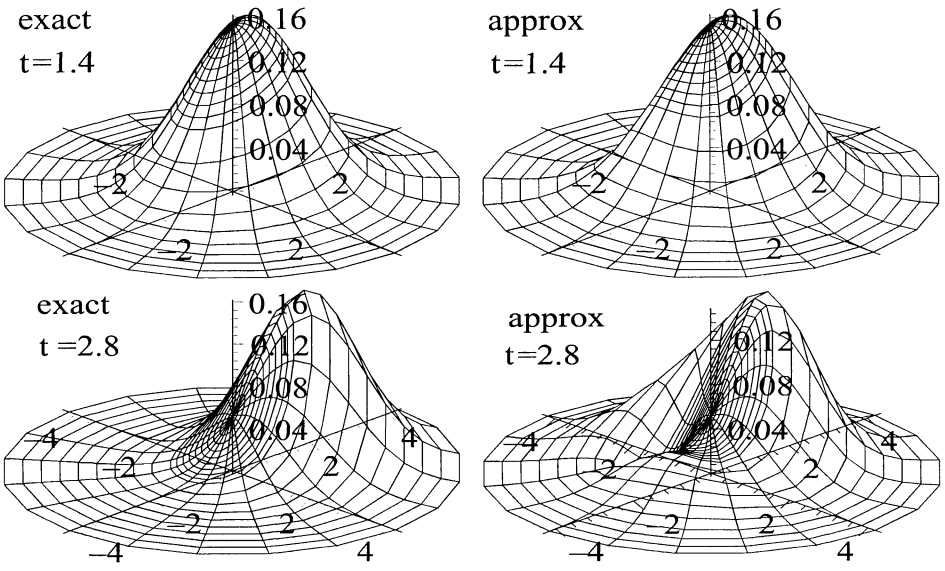

Figure 1: The dynamics of the eigenfunction of a two-dimensional oscillator . See comments in the text.

4. NUMERICAL RESULTS

4.1. Two-dimensional oscillator

In Table 1 we show the discrepancy $Er(t) \equiv Er(t, 1)$ between the exact and numerical solutions determined by Eq. (76) at the time step $\delta t = 0.0025$ (See Section 2.1 and Eqs. (23), (24)) versus N and $t = T$; t_{run} is the run

Table 2. The values $\alpha(\tau)$ and $Er(\tau, j)$ for the Crank-Nicholson scheme at first six kicks. Here $\delta\tau = \hat{T}/64$, $n = 5$, l_{max}=6 and ρ_{max}=80

N	1	2	3	4	5	6
$Er(\tau, 1)$	0.17123	0.34128	0.50887	0.67243	0.83054	0.98214
$Er(\tau, 2)$	0.04128	0.08258	0.12389	0.16510	0.20612	0.24689
$Er(\tau, 3)$	0.00828	0.01658	0.02491	0.03320	0.04146	0.04971
$\alpha(\tau)$	1.97713	1.97072	1.95963	1.94354	1.92303	1.89869

time (in minutes) of the computer calculations for the considered example of $a_1 = 0.6$, $a_2 = 0.4$, $\omega = 1$, $\omega_1 = 0.8$, $\omega_2 = 1.2$, solved by means of the Crank-Nicholson scheme of the second-order accuracy in the time step δt, and $R(t) = \sqrt[4]{1 + \gamma^4 t^4}$, $\gamma^2 = 0.1$. To approximate the solution $\xi_j(\rho, \tau)$ in the spatial radius ρ we used the finite element grid $\Omega_\rho = \{\rho_{min} = 0, (100), 1, (300), \rho_{max} = 10\}$, where the number in the brackets denotes the number of finite elements in the intervals. Between each two nodes we apply the Lagrange interpolation polynomials up to the fourth order. One can see that the discrepancy $Er(T)$ decreases with increasing number N of equations at the fixed time interval T and increases with the time interval T at a fixed number of equations $N_{max} = N$.

In Fig. 1 the eigenfunction of the oscillator (27) (exact) and its Galerkin projection (17) with $N = 15$ (approx) are shown. At small t the wave packet goes away from the origin of coordinates; therefore, for its description at increasing T a larger number of equations is needed.

Indeed, a number of transitions to the unaccounted states $k > N$ grows in time t, meanwhile an upper bound $N < N_{max}$ can be estimated because the wave packet propagation Eq. (27) is localized in a finite spatial region. It means that one can reveal such parameterization of the external fields $E_1(t)$, $E_2(t)$ that leads to transitions into prescribed states with the maximal probability at a time interval T and solve the problem of control of the quantum system under consideration[12] . To reduce the run time t_{run} needed for more effective computer simulation the splitting algorithms should be applied based on the appropriate approximations of both the evolution operator and external fields.

4.2. Three-dimensional Coulomb atom

We use the enclosed time grid for the first six kicks with the step $\delta\tau$ and examine the behaviour of the function $Er(\tau, j)$ (72). For the function $\chi_l^n(\rho, \tau)$, the approximate calculation with time step $\delta\tau/8$ can be used. By means of these values $Er(\tau, j)$ we can calculate the convergence rate $\alpha(t)$ of the calculation schemes (67) and (68) by means of the formula (73). To approximate the solution $\chi_l^n(\rho, \tau)$ in the spherical radius ρ we used finite-element grid $\Omega_\rho = \{\rho_{min} = 0, (50), 10, (100), \rho_{max} = 80\}$. Between each two nodes we apply the Lagrange interpolation polynomials of the sixth order.

In Tables 2 and 3 we show the values $\alpha(\tau)$ and $Er(\tau, j)$ determined by Eq. (72) for the Cranck-Nicholson and implicit fourth-order schemes at the first six kicks with the field period $T = 5357t_0$, field strength $F = 2 \times 10^{-3}$, $n = 5$, l_{max}=6 and ρ_{max}=80. Here $\delta\tau = \hat{T}/64$ for the Cranck-Nicholson scheme and $\delta\tau = \hat{T}/16$ for the implicit fourth-order scheme. Fig. 2 shows: a) the probabilities $P_{n=9} = \sum_{l=0}^{8} |\langle 9, l, 0|\psi(t)\rangle|^2$ and $P_{n=10} = \sum_{l=0}^{9} |\langle 10, l, 0|\psi(t)\rangle|^2$ with $|\psi(0)\rangle = |n = 9, k = 0, m = 0\rangle$, b) the autocorrelation function $|\langle\psi(t)|n = 9, k = 0, m = 0\rangle|$, c) the autocorrelation function $|\langle\psi(t)|n = 9, l = 0, m = 0\rangle|$ depending on the number of kicks, and d) the expectation value of the angular momentum $\langle l\rangle(t)$ for the initial wave packet $|\psi(0)\rangle = |n = 9, l = 0, m = 0\rangle$.

In the case of the magnetic field with strength β parallel to the z axis an additional quadratic Zeeman term V_Z should be added to H_0, i.e.

$$H_0 = -\frac{1}{2}\Delta_{\vec{\rho}} - \frac{n}{\rho} + V_Z, \quad V_Z = \frac{1}{8} n^4 \beta^2 \rho^2 \sin^2\theta, \tag{77}$$

Table 3. The values $\alpha(\tau)$ and $Er(\tau, j)$ for the implicit fourth-order scheme at first six kicks. Here $\delta\tau = \hat{T}/16$, $n = 5$, l_{max}=6 and ρ_{max}=80

N	1	2	3	4	5	6
$Er(\tau, 1)$	0.07030	0.14070	0.21122	0.28125	0.35029	0.41848
$Er(\tau, 2)$	0.00473	0.00954	0.01441	0.01921	0.02395	0.02862
$Er(\tau, 3)$	0.00028	0.00097	0.00176	0.00199	0.00183	0.00198
$\alpha(\tau)$	3.88197	3.93554	3.96044	3.92720	3.88293	3.87135

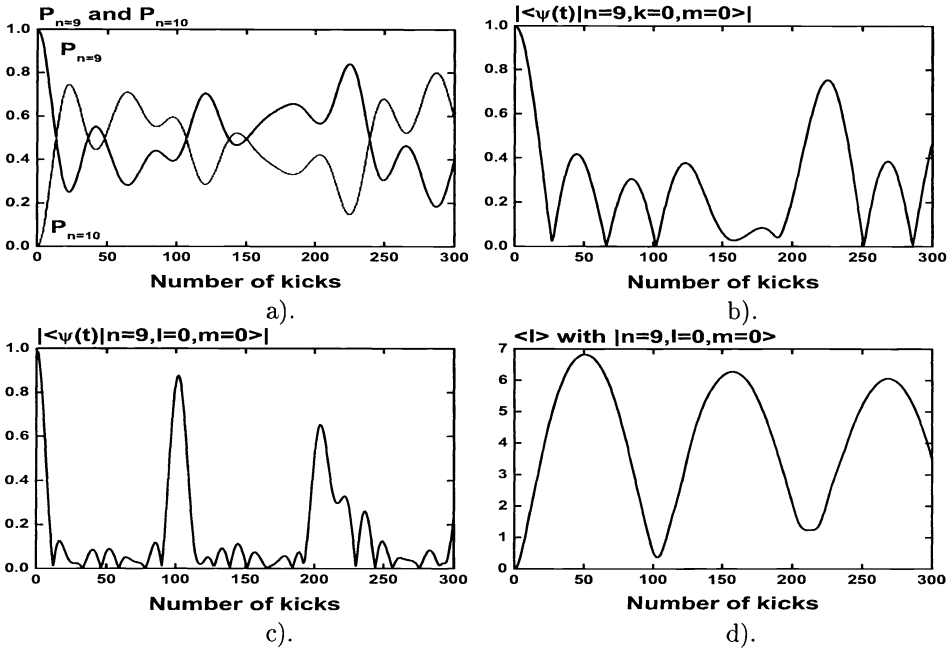

Figure 2: The dynamics of physical quantities of a kicked hydrogen atom. See comments in the text.

then the diagonal $H_{ll}^{(0)}$ and nondiagonal $H_{ll'}^{(0)}$ matrix elements in the equation (41) have the form

$$H_{ll}^{(0)}(\rho) = \frac{l(l+1)}{2\rho^2} - \frac{n}{\rho} + \frac{n^4\rho^2\beta^2}{8}\left(1 - \frac{(l+1)^2}{4(l+1)^2-1} - \frac{l^2}{4l^2-1}\right)$$
$$H_{ll'}^{(0)}(\rho) = -\frac{n^4\rho^2\beta^2}{32\sqrt{(2l+1)(2l'+1)}}\frac{(l+l'+1)^2-1}{(l+l'+1)}\delta_{2,|l'-l|}. \tag{78}$$

Table 4 shows the multiplet $|n, \nu = 0...n-1, m\rangle$ of the energy eigenvalues at $n = 9$ with $\beta = 0.002$ and the comparison with the first-order perturbation corrections. Fig. 3 shows: a) the probabilities $P_{n=9} = \sum_{l=0}^{8} |\langle 9, l, 0|\psi(t)\rangle|^2$ and $P_{n=10} = \sum_{l=0}^{9} |\langle 10, l, 0|\psi(t)\rangle|^2$, b) the autocorrelation functions $|\langle\psi(t)|\psi(0)\rangle$ and c) the expectation values of the angular momentum $\langle l\rangle(t)$ for the initial Zeeman wave packets $|\psi(0)\rangle = |9, v = 0, 0\rangle$ (l.h.s) and $|\psi(0)\rangle = |9, v = 8, 0\rangle$ (r.h.s) depending on the number of kicks.

5. CONCLUSIONS

Stable numerical splitting schemes for solving the TDSE, possessing high accuracy with respect to both variables t, x, are developed. New results are obtained for the long-range-potential TDSE with the magnetic field and a train of ultra-short laser pulses, approximated by a set of δ-function kicks, using a PC without essential

Table 4. The eigenvalues E_{calc} of the Zeeman states $n = 9, v, m = 0$ of the hydrogen atom in the constant magnetic field $\beta = 0.1472(-4)$ calculated for the set of $l = 0, \cdots, 9$ spherical functions, $\delta E_{calc} = (E_{calc} - E^{(0)})/\beta^2$ corresponds to the first-order corrections $E_{pt}^{(1)}$ found by means of the perturbation calculation $E_{pt} = E^{(0)} + \beta^2 E_{pt}^{(1)}$. Below the factor x in the brackets means $(x) \equiv 10^x$.

v	E_{calc}	E^0	δE_{calc}	E_{pt}^1
0	-6.172 798(-3)	-6.172 839 (-3)	1529.11	1529.16
1	-6.172 797(-3)	-6.172 839 (-3)	1545.01	1545.04
2	-6.172 747(-3)	-6.172 839 (-3)	3384.07	3384.10
3	-6.172 728(-3)	-6.172 839 (-3)	4080.42	4080.47
4	-6.172 689(-3)	-6.172 839 (-3)	5536.15	5536.38
5	-6.172 641(-3)	-6.172 839 (-3)	7315.02	7315.33
6	-6.172 582(-3)	-6.172 839 (-3)	9476.34	9476.83
7	-6.172 514(-3)	-6.172 839 (-3)	12006.50	12007.13
8	-6.172 435(-3)	-6.172 839 (-3)	14902.72	14903.51

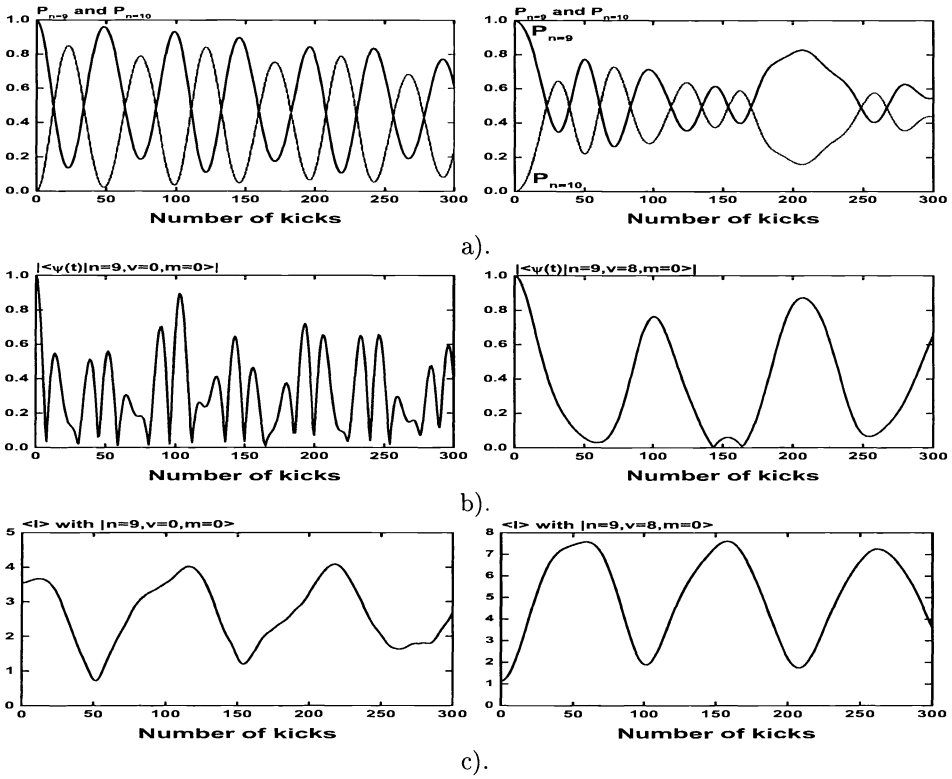

Figure 3. The dynamics of physical quantities of the kicked hydrogen atom in the uniform magnetic field. See comments in the text.

computer resources. The approach proposed in this paper opens the way to apply the elaborated methods to solving the TDSE for the system of second-order ordinary differential equations generated by the Galerkin and Kantorovic methods for multidimensional problems[11] . The problems to which the proposed technique can be applied include nonstationary phenomena in near-resonance self-action of modulated beams and ultra-short pulse propagation in nonlinear absorbing and dispersive media.

6. ACKNOWLEDGMENT

This work was partially supported by the grant No. 03-02-16263 from the Russian Foundation for Basic Research, the contract No.40.018.1.1.1314 with the Russian Ministry of Industry, Science and Technologies, and the grant from the President of the Bulgarian State Agency for Atomic Energy (2003).

REFERENCES

1. V.L. Derbov, L.A. Melnikov, I.M. Umansky, and S.I.Vinitsky. Phys. Rev. **55**, 1997, p.3394.
2. I.M. Umansky, L.A. Melnikov, V.L. Derbov, M.V. Ryabinina, S.I. Vinitsky. Phys. Atomic Nuclei **61**, 1998, p.1928-1931.
3. Yu.V. Popov, K.A. Kouzakov, A.A. Gusev, S.I. Vinitsky, Model of interaction of zero-duration laser pulses with an Atom. Proc. SPIE, V.L. Derbov, L.A. Melnikov, L.M. Babkov (Eds.), v. 5069, pp.33-42, 2003.
4. V.L. Derbov, M.S. Kaschiev, V.V. Serov, A.A. Gusev, S.I. Vinitsky, Adaptive numerical methods for time-dependent Schroedinger equation in atomic and laser physics. Proc. SPIE, V.L.Derbov,L.A. Melnikov, L.M. Babkov (Eds.), v. 5069, pp. 52-60, 2003.
5. G.I. Marchuk, On the theory of splitting-up method in "Partial Differential Equations. II SYNSPADE-1970", Academic Press, N.Y.,L. 1971.
6. I.V. Puzynin, A.V. Selin, S.I.Vinitsky, Comput. Phys. Commun. **126**, 2000, p.158-161.
7. N.G. Bankov, M.S. Kaschiev, S.I. Vinitsky, Comptes rendus de l'Akademie bulgare des Scienses **55**, 2002, pp. 25-30.
8. G. Strang & G. Fix. An Analisys of The Finite Element Method, Printice-Hall, Englewood Cliffs. N.J., 1973.
9. K. J. Bathe, Finite Element Procedures in Engineering Analysis, Englewood Cliffs, Prentice Hall, New York, 1982.
10. A.G. Abrashkevich, D.G. Abrashkevich, M.S. Kaschiev, I.V. Puzynin, Comput. Phys. Commun., **85**, 1995, p.10, p.65.
11. A.G. Abrashkevich, M.S. Kaschiev and S.I. Vinitsky. J. Comput. Physics, **163**, 2000, p.328.
12. A.G. Butkovskiy, Yu.I. Samoilenko. Control of Quantum-Mechanical Processes and Systems, Kluwer Academic Publishers, Dordrecht Hardbound, ISBN 0-7923-0689-9 1990, 240 pp.
13. M. Klews, W. Schweizer, Phys. Rev. A, **64**, 2001, pp. 053403-1-053403-5.
14. C.B. Tarter, Coefficients connected the Stark and fieldfree finctions for Hydrogen J. Math. Phys. **11**, 1970, pp. 3192–3195.
15. A. H. Stroud, Approximate Calculation of Multiple Integrals, Prentice Hall, Englewood Cliffs, 1971.
16. K.Fletcher Numerical methods on basis of Galerkin's approach, M. Mir, 1988.